Nat. Hazards Earth Syst. Sci. Discuss., 1, 7239–7269, 2013
www.nat-hazards-earth-syst-sci-discuss.net/1/7239/2013/
doi:10.5194/nhessd-1-7239-2013

Natural Hazards
and Earth System
Sciences
Discussions
Open Access

# Temporal variations in the wind and wave climate at a location in the eastern Arabian Sea based on ERA-Interim reanalysis data

**P. R. Shanas and V. Sanil Kumar**

Ocean Engineering, CSIR-National Institute of Oceanography (Council of Scientific and Industrial Research), Dona Paula, Goa 403 004, India

Received: 30 October 2013 – Accepted: 18 November 2013 – Published: 6 December 2013

Correspondence to: V. Sanil Kumar (sanil@nio.org)

Published by Copernicus Publications on behalf of the European Geosciences Union.

## Abstract

Temporal variations of wind speed and significant wave height (SWH) at a location in the eastern Arabian Sea is studied using ERA-Interim reanalysis data during 1979–2012. A Shallow water location is selected for the study since measured buoy data is available close to the location for comparison of the reanalysis data. Annual mean wind speed shows a statistically significant decreasing trend of 1.5 $\text{cm}\,\text{s}^{-1}\,\text{yr}^{-1}$. Weakening of SWH during one of the peak monsoon month (August) is identified from the monthly analysis of SWH, which shows higher upward trend in SWH during south west monsoon period with an exception during August. The annual mean SWH shows slight upward trend (0.012 $\text{cm}\,\text{yr}^{-1}$), whereas larger upward trend (1.4 $\text{cm}\,\text{yr}^{-1}$) is observed for annual maximum SWH. The influence of tropical cyclone activity is also studied and found that the maximum SWH and wind speed during 1996 is directly related to the cyclonic event. The relationship between annual maximum wave height and wind speed with ENSO and Indian Ocean Dipole (IOD) are tested and found that larger waves are reported during strong El-Niño and negative IOD year, whereas decrease in maximum wave height and wind speed is observed during strong La-Niña and positive IOD year.

## 1 Introduction

Knowledge of the wind and wave climate is required for engineering design (e.g. ships and offshore platforms) and shipping industry (Krogstad and Barstow, 1999; Tucker and Pitt, 2001). Wind and wave climate is assessed based on the data obtained through (i) in-situ measurement, (ii) model dataset, (iii) satellite altimeter and (iv) voluntary observing ship (VOS) data. Understanding the long-term variations in the wind and wave parameter is a key element in contemporary physical oceanography and coastal science. Long-term wind and wave records based on in-situ measurements are still sparse in the Arabian Sea (AS) and only short-term records are available (Premkumar et al., 2000; Kumar, 2006; Sajiv et al., 2012; Glejin et al., 2013). A comprehensive understanding of the properties of the approaching waves and their potential changes are the major knowledge necessary for sustainable management of both offshore activities and the coastal region (Soomere and Räämet, 2011). Generally significant wave height (SWH) is used to study the wave climate at a location. Globally there have been many studies on the change in wave climate especially in north Pacific and north Atlantic region (Carter and Draper, 1988; Allan and Komar, 2000; Caires and Swail, 2004; Gulev and Grigorieva, 2004; Soomere and Räämet, 2011; Vanem and Walker, 2013). Kumar and Sajiv (2010) carried out a study on variations in long-term wind speed estimates considering different decades in the AS and reported that extreme wind speed has an annual decreasing trend of 1.3 $\mathrm{cm\,s^{-1}}$.

As a part of the global study, Caires and Swail (2004) examined the long-term trend in SWH in the AS based on VOS data. But the long-term changes and decadal variation in wave climate in the eastern AS is not known at present. Since no regionalized study has been done on the temporal variations of SWH in the eastern AS, a study is carried out using ERA-Interim re-analysis dataset. The objective of the study is to quantify the monthly, inter-annual and decadal variability of the wind and wave climate at a location in the eastern AS. The analysis is based on the wind speed and SWH data obtained from ECMWF reanalysis ERA-Interim data for 34 yr (1979–2012). Shallow water location (14.25° N, 74.25° E) in the eastern AS is selected for the study since measured buoy data is available close to this location for comparison of the ERA-Interim SWH data (Fig. 1).

## 2 Data and methodology

### 2.1 ERA-Interim reanalysis data

Present study is based on the ERA-Interim global atmospheric reanalysis data which are produced by European Center for Medium-Range Weather Forecasts (Berrisford et al., 2009; Dee et al., 2011). ERA-Interim is the first re-analysis using adaptive and fully automated bias corrections of satellite radiance observations (Dee and Uppala, 2008) and contains improvements on ERA-40 such as the complete use of four-dimensional variational data assimilation. Wind speed and SWH are downloaded for the period from January 1979 to December 2012 at 6 hourly intervals with a resolution of 0.75° × 0.75° latitude/longitude and used in the study. Wind speeds are derived from the zonal and meridional component of winds at 10 m a.s.l. We studied monthly variation in parameters (wind speed and SWH) by creating monthly data from the 6 hourly data and taking the mean of those months over a period of 34 yr.

## 2.2 Buoy data

Measured wave data at 9 m water depth (14.304° N, 74.391° E) off Honnavar (Fig. 1) using a moored directional wave rider buoy during January 2011–December 2012 is used in the present study for comparison of the ERA-Interim SWH data. From the heave data recorded by the buoy for 30 min duration at 1.28 Hz interval, the wave spectrum is obtained through Fast Fourier Transform (FFT). FFT of 8 series, each consisting of 256 measured heave data of the buoy, are added to obtain the spectrum. The high frequency cut-off is set at 0.58 Hz and the resolution is 0.005 Hz. SWH is obtained from the wave spectrum.

## 2.3 Comparison of reanalysis data with measured data

Extensive inter comparison and evaluation of wind stress estimates from reanalysis dataset (ERA-Interim) against available in-situ observations are done for the tropical Indian ocean (Praveen et al., 2013). Evaluation of the data is based on the comparison with available observations from the global tropical moored buoy array (McPhaden et al., 1998) and OceanSITES (http://www.OceanSITES.org, 2009) data with observations and reported that ERA-Interim data captures well temporal variability with better performance (∼ 0.86 correlation). For the present study, the nearest

Title Page
Abstract Introduction
Conclusions References
Tables Figures
◀ ▶
◀ ▶
Back Close
Full Screen / Esc
Printer-friendly Version
Interactive Discussion

available ERA-Interim SWH data to the measured in-situ buoy data at Honnavar during 2011 and 2012 are used for the comparison. The comparison between the reanalysis and measured SWH data shows very high correlation (correlation coefficient = 0.96) with small RMS error (0.27 m) during both years. Scattering Index (SI) value is 0.23 with a positive bias of 0.2 m during 2011 whereas slightly reduced SI and bias is observed during 2012 (Fig. 2).

## 3 Results and discussions

### 3.1 Variation in wind speed during 1979–2012

Temporal variation of monthly maximum and mean wind speed is plotted for 34 yr (Figs. 3 and 4). Monthly maximum wind speed show a decreasing trend during February–April, June–August and in October (Table 1). Other months show upward trend in monthly maximum wind speed. The monthly mean wind speed show a decreasing trend in all months with higher values during the peak south west monsoon season (June and August). Even though, a higher decreasing trend (~ 4 $\mathrm{cm\,s^{-1}\,yr^{-1}}$) of mean wind speed is observed during August, the decreasing trend is less (0.079 $\mathrm{cm\,s^{-1}\,yr^{-1}}$) for maximum wind speed (Table 1). The highest upward trend in maximum wind speed is observed during September (6.14 $\mathrm{cm\,s^{-1}\,yr^{-1}}$).

Upward trend (3.6 $\mathrm{cm\,s^{-1}\,yr^{-1}}$) is observed for annual maximum wind speed and a decreasing trend (1.5 $\mathrm{cm\,s^{-1}\,yr^{-1}}$) is observed for annual mean wind speed (Fig. 5). The difference in trends for annual maximum and mean wind speed is due to the fact that, individual events would drive the trends of annual maximum and statistically that becomes meaningless. The annual maximum and mean wind speed during 1979 to 2005 has a decreasing trend of 1.4 and 0.8 $\mathrm{cm\,s^{-1}\,yr^{-1}}$ respectively. The overall negative trend in maximum wind speeds is shifted to positive by individual events in 2006 and 2007. During June 2006, high wind speed is observed with the onset of the southwest monsoon (Sanil Kumar et al., 2010). High wind speed observed in

June 2007 is due to the remnant of a deep depression which developed over west central Bay of Bengal (BoB) on 21 June and moved west-northwestwards across south India during 22–23 June emerged into northeast AS as a well marked low pressure area on 24 June. Hence we have estimated the 90th and 99th percentile winds which still provide enough data point for stronger winds (which drive most of the wave action) to carry out a relevant statistical analysis. The 90th and 99th percentile values show decreasing trend (1.9 and 1.6 $\mathrm{cm\,s^{-1}\,yr^{-1}}$) similar to the trend of annual mean wind speed (1.5 $\mathrm{cm\,s^{-1}\,yr^{-1}}$).

Statistical analysis of wind speed frequency is done by classifying wind speed into different range through decadal period during (i) 1980–1989, (ii) 1990–1999 and (iii) 2000–2009 (Table 2). The study shows a decreasing trend in frequency of occurrence of stronger wind. The weakening of strong winds can be also evident from the decreasing trend of monthly mean wind speed over 34 yr.

Study on long-term variation of wind speed by Kumar and Sajiv (2010) along the AS considering different decades reported that extreme wind speed has an annual decreasing trend of 1.3 $\mathrm{cm\,s^{-1}}$. Some other studies also indicated declining trend of wind speed in the last decade around the globe (Jiang et al., 2010). The decrease in frequency of occurrence of stronger wind (90th and 99th percentile) in the present study also supports the fact that the cyclonic activity in the AS is decreasing. Based on 118 yr period data of cyclonic disturbances including cyclonic storms in AS, Shyamala and Iyer (1996) examined the decadal variability and found that maximum number of cyclonic storms in AS occurred during the decade 1901–1910 (15) followed by 1961–1970 (14), 1971–1980 (13), 1981–1990 (3) and 1991–2000 (7). The decade 1981–1990 had the lowest frequency (3) of cyclonic storm and severe cyclonic storm. These are statistically significant decadal variability with decreasing tendency in decadal frequency of cyclonic storms in AS since the last 3 decades from 1971–2000. Srivastava et al. (2000) studied trends in annual cyclonic disturbances for the period 1891–1997 over the BoB and the AS and found that there is a significant decreasing trend in the annual frequency of storms over both the basins and the slopes of decreasing trend are maximum during the last four decades. Singh (2001) examined the long-term trend in the frequencies of cyclonic disturbances (depression) and the cyclonic storms forming over the BoB and the AS in monsoon season and found that frequency of cyclonic disturbances has decreased at a rate of about 6–7 disturbances per hundred years whereas frequency of cyclonic storms has decreased at the rate of about 1–2 cyclonic storms per hundred years.

### 3.2 Variation in significant wave height during 1979–2012

Monthly mean and maximum value of SWH for 34 yr are presented in Figs. 6 and 7. Higher wave heights observed during the SW monsoon months are in line with the observation on monsoon wind speed and the earlier studies on waves in AS (Kumar et al., 2000, 2003, 2012; Sajiv et al., 2012; Glejin et al., 2013). The monthly mean SWH shows decreasing trends in August and from November to April, whereas during other months upward trend is found. SW monsoon period showed higher upward trend in mean SWH with an exception during August and maximum upward trend is observed during September ($0.9\,\mathrm{cm\,yr^{-1}}$). The significant weakening of strong winds during August also reflects the cause of weakening of mean SWH. Whereas, the monthly maximum SWH shows an upward trend for most of the months except during February–April. The decreasing trend during February–April is observed in the range $0.15$–$0.37\,\mathrm{cm\,yr^{-1}}$. During SW monsoon season, the monthly maximum SWH showed a higher upward trend, with maximum during September ($1.9\,\mathrm{cm\,yr^{-1}}$) similar to the mean SWH.

The annual mean SWH show slight upward trend with an increase of $0.012\,\mathrm{cm\,yr^{-1}}$, whereas an increasing trend of $1.4\,\mathrm{cm\,yr^{-1}}$ is observed for annual maximum SWH (Fig. 8). The trend in annual maximum SWH depend on individual events and hence the 90th and 99th percentile values of SWH are estimated. The 90th and 99th percentile values of SWH increased by 0.15 and $0.76\,\mathrm{cm\,yr^{-1}}$ respectively (Fig. 8). The increase in annual mean is much lower than the 90th and 99th percentile and the annual maximum values, suggesting larger positive trends for higher waves. Higher rate of increase for

99th and annual maximum SWH indicate that extremes are increasing at a faster rate than the mean. Since the annual mean, maximum and the 90th and 99th percentile SWH have the increasing trend, the study shows that the SWH has a increasing trend at the location studied.

Similar results of increasing trend in SWH can be observed in the study of Hemer et al. (2010) for Indian Ocean sector of Southern Ocean. Gulev and Grigorieva (2004) studied over 100 yr of ship observations and reported slightly increasing trend in mean wave height of 0.14 m decade$^{-1}$ for the North Atlantic and 0.08–0.1 m decade$^{-1}$ for the North Pacific. Neu (1984) and Bouws et al. (1996) analyzed synoptic charts issued by the Meteorological and Oceanographic Center (Canada) for the North Atlantic and largely based on ship observations. They found a trend in average wave height of 0.23 m decade$^{-1}$ (1970–1982) whereas Neu (1984) reported larger values between 0.6 and 1.4 m decade$^{-1}$ (1960–1985). More recent studies of buoy data in the North Pacific has shown increasing trends in average SWH between 0.05 and 0.27 m decade$^{-1}$ during 1979–1999 (Allan and Komar, 2000) and 0.15 m decade$^{-1}$ for the period 1976–2007 (Ruggiero et al., 2010; Young et al., 2011).

The present study shows that at the study location, the mean, 90th and 99th percentile wind speed have a decreasing trend whereas the corresponding SWH have a increasing trend. This contrasting result is due to the fact that waves in the eastern Arabian Sea are mainly the swells propagating from south Indian Ocean and southern Ocean (Glejin et al., 2013; Sajiv et al., 2012) and hence are not directly related to the local phenomenon. Hemer et al. (2013) reported that increased Southern Ocean wave activity influence a larger proportion of the global ocean as swell propagates northwards into the other ocean basins (Hemer et al., 2013). The increase in swells at the study location is also evident from the increase in wave period (Fig. 9). The increase in swells at the study location is due to the increase in wind speed over the southern ocean during the past 20 yr as observed by Young et al. (2011).

### 3.3 Intensity of wind speed and wave height during the peak events in AS

Wave climate of the AS and that along the west coast of India mainly depends on the wind conditions prevailing during SW monsoon (June–September), north east monsoon (October–January) and pre monsoon (February–May) (Glejin et al., 2013). Winds during the SW monsoon produce high wave activity (SWH $> 1.5$ m) and relatively calm condition (SWH $< 1.5$ m) prevails during the rest of the year. Stronger storm events like cyclone produce higher waves in the region. Gray (1985) found that north Indian Ocean accounts for 7 % of global tropical cyclones. Occurrences of tropical cyclones are more in the BoB than in the AS, and the ratio of their frequencies is about 4 : 1 (Dube et al., 1997). During 1979–2008, there has been an average of 4.7 cyclonic storm days per year over the AS with 1981, 1990, 1991, 2000, 2005, 2008 having 0 storms; and 1998 and 2004 having more than 15 cyclonic storm days (Evan and Camargo, 2010 ). Hence, to examine the influence of these cyclonic events on the waves, the extreme SWH during the study period are analysed. During 1979–2012, there are 3 peak events with SWH more than 4.5 m; peak1 in 1989, peak2 in 1996 and peak3 in 2000. During 1989, 1996 and 2000, the occurrence of cyclone is observed along the west coast of India. During 1989, tropical cyclone 02A developed off the west coast of India from 7–13 June with wind speed upto 15.3 $\mathrm{m\,s^{-1}}$ (30 mph) but the peak1 is on 23 July and is not due to the cyclone period (7–13 June). In 1996, a tropical depression formed in the AS from 9–12 June and developed into a tropical storm on 17 June off the west coast off India. This severe cyclonic storm during 17–20 June had peak intensity of 30.6 $\mathrm{m\,s^{-1}}$ and generated the peak2 event. During 2000, a depression formed at BoB, on 26 November and intensified into a storm and crossed the Indian sub-continent. But the peak3 is on 7 June and not during the cyclone period (26–30 November). Simon et al. (2001) found an increase in wind speed over the AS off Karnataka coast on 6–7 June based on the multi frequency microwave radiometer study. The increase in the local wind speed during 6–7 June is the reason for unusual increase in SWH during the peak3 event.

### 3.4 Influence of ENSO and Indian Ocean dipole on wind and waves

During the three peak events, the SWH observed are 4.8, 5.5 and 5.4 m and the wind speed observed are 14.0, 14.1 and 16.5 $\mathrm{m\,s^{-1}}$ respectively. The most logical cause of the peak identified in the wave height might be due to the increase in wind speeds over time. When the wave height is compared with the cyclonic events in the previous section, it is clear that they are not directly related for all three events. Maximum SWH during the peak2 event is only during the cyclonic event (Fig. 10) and the high SWH observed during peak1 and peak3 are not due to the cyclonic storm. This finding is not surprising since the wave climate in AS region is also influenced by the distant storms (Glejin et al., 2013). ENSO and Indian Ocean dipole (IOD) are two dominant modes of climate variations in the tropical Pacific and Indian Oceans. Both modes are shown to influence the climate conditions of several parts of the world. Some studies noticed the influence of Tropical cyclone (TC) activity on IOD mode (Saji et al., 1999; Webster et al., 1999), which in turn influences the wind pattern and can be clearly seen as high energy waves since the wind and waves are correlated. Also it is seen in literature that North Indian Ocean TC activity is notably influenced by the IOD mode. When the Indian Ocean is in a positive (negative) phase of the IOD, North Indian Ocean SST (sea surface temperature) anomalies are warm in the west (east) and cold in the east (west), which can weaken (strengthen) convection over the BoB and eastern AS, and cause anticyclone (cyclonic) atmospheric circulation anomalies at low levels. This result in less (more) TC genesis and reduced (increased) opportunities for TC occurrence in the North Indian Ocean (Yuan and Cao, 2012). Webster et al. (1999) indicated that IOD events are tied to strongly coupled ocean-atmosphere-land interactions, and are important in Indian-Pacific regional climate variations. On the other hand, ENSO, is a coupled ocean-atmosphere phenomenon of the tropical Pacific, also show significant effects on tropical cyclone as well as in climatic signals in Indian Ocean region (Jury, 1993; Reason et al., 2000).

To extend the argument for a relationship between the IOD, ENSO with observed SWH and wind speed in the AS, the annual average maximum SWH and wind speed is correlated with the IOD and ENSO indices. An IOD event can be detected using Dipole Mode Index (DMI) which is defined as the difference in SST anomalies between western and eastern equatorial Indian Ocean. The oceanic Nino index (ONI) is used for identifying El-Niño (warm) and La-Niña (cool) events in the tropical Pacific. It is the running 3 month mean SST anomaly for the Niño 3.4 region (5° N–5° S, 120–170° W). Events are defined as 5 consecutive months at or above the +0.5° anomaly for warm (El-Niño) events and at or below the −0.5° anomaly for cold (La-Niña) events. The threshold is further broken down into weak (with a 0.5–0.9° SST anomaly), moderate (1.0–1.4°) and strong (≥ 1.5°) events. For determining the El-Niño/La-Niña and positive/negative IOD years, we have downloaded Nino 3.4 index and IOD mode index from the NOAA and JAMSTEC websites and both of ONI and dipole mode indices were overlaid to one graph (Fig. 10c). We have analysed DMI and Nino 3.4 index with SWH and wind speed (Fig. 10a and b) and found that during the peak events (peak1 and peak2), the Nino 3.4 index and DMI shows high negative trend. During a positive IOD year, the eastern Indian Ocean is colder than normal while the western Indian Ocean is warmer than normal. Since the DMI is defined as a difference between the western box and the eastern box, the index is positive during a positive IOD year and is negative during negative IOD year. It has been noted that ENSO remote forcing leads to an Indian Ocean basin scale warming in the following spring after the ENSO matures (Xie et al., 2002). Nearly 40 % of IOD occurs simultaneously with ENSO; the positive IOD is associated with El-Niño and the negative IOD generally with La-Niña (Saji and Yamagata, 2003; Ashok et al., 2004). After carefully observing the pattern of these two index with yearly maximum SWH and wind speed, it is found that, during certain years when both the index shows positive value, the SWH is found to be less. The co-occurrence of both events, positive IOD events (Yamagata et al., 2002; Vinayachandran et al., 2007) and El-Niño can be observed in many years (1982, 1991, 1994 and 1997) noted as phase 1. The co-occurrence of negative IOD events

(Meyers et al., 2007) and La-Niña can also be observed during 1989 and 1998 noted as phase 2. During phase 1, 1982, 1994 and 1997 are strongest positive IOD years, an anticyclonic atmospheric circulation at low level can be observed (Yuan Junpeng and Cao Jie, 2012) which in fact reduces the cyclonic occurrence over AS. Significant reduction in the maximum wind speed and maximum SWH can be observed during this period. Also in reverse, extreme SWH and wind speed are observed during phase 2 (1989 and 1998).

### 3.5 Statistical trend analysis for the time series data

A statistical analysis of the ERA-Interim wave and wind time series has been performed to test the significance of trends during the 34 yr period. A Student's *t* test and *z* test have been used to assess the probability distribution with N-1° of freedom with level of significance ($\alpha$) fixed at 5 %. The result of the *t* test and *z* test are presented in Table 3. The null hypothesis of zero-slope is rejected for all the parameter at a 5 %-level of significance. For all parameter as the computed *p* value for *t* test and *z* test is lower than the significance level $\alpha = 0.05$, one should reject the null hypothesis H0, and accept the alternative hypothesis Ha (Where H0: the difference between the means is equal to 0, Ha: the difference between the means is different from 0). There are several statistical tests available for testing the time series data (Hirsch et al., 1993). These tests start from a null hypothesis that the observations are samples from a stationary process. The likelihood of this hypothesis is evaluated based on the value of a test statistic, a property of the data set. A *p* value of 5 % is a common critical value for accepting statistical significance, but there is no reason why other values cannot be used. Rejection of the null hypothesis at the 5 % significance level means that we are 95 % confident of non-stationary. The Mann–Kendall test is a non-parametric significance test for a monotonic trend in a time series based on the Kendall's tau ($\tau$) (Mann, 1945; Kendall, 1975). We have carried out a two tailed Mann–Kendall test with the linear fitted trend for the long-term trend of annual wave and wind parameter. The result is presented in Table 4. As the computed *p* value is lower than the significance level alpha=0.05, one should reject the null hypothesis H0, and accept the alternative hypothesis Ha, (where Ha: there is a trend in the series, H0: there is no trend in the series). Statistically significant trend is found for wind speed and wave period mean trends, the null hypothesis of zero-slope is rejected for this cases at a 5 %-level of significance. The Theil–Sen slope (Sen, 1968; Theil, 1950), also known as "Kendall's slope" or the "Nonparametric linear regression slope", is an alternative to the standard linear regression slope. Theil Sen's slope estimate is also is method for robust linear regression that chooses the median slope among all lines through pairs of two-dimensional sample points. Positive and negative value in Sen's slope indicates positive and negative trend respectively.

## 4 Conclusions

Long-term trend in wind and wave along the eastern AS is analysed using ERA-interim dataset. The study shows that during 1979–2012, the annual mean wind speed shows a decreasing trend (1.5 $\mathrm{cm\,s^{-1}\,yr^{-1}}$) whereas the annual maximum wind speed showed an upward trend of 3.6 $\mathrm{cm\,s^{-1}\,yr^{-1}}$. The annual maximum and average wind speed during 1979–2005 has a decreasing trend of 1.4 and 0.8 $\mathrm{cm\,s^{-1}\,yr^{-1}}$ respectively. The higher wind speed associated with the local depression events occurred in AS during 2006 and 2007 shifted the trend of annual maximum wind speed during 1979 to 2012 from negative to positive. During the SW monsoon period higher upward trend in significant wave height (SWH) is observed with an exception during August. Annual mean SWH show small increasing trend (0.012 $\mathrm{cm\,yr^{-1}}$), whereas higher increasing trend of 1.4 $\mathrm{cm\,yr^{-1}}$ is observed for annual maximum SWH. Detailed analyses have been carried to examine the influence of the cyclonic events on the intensity of wave activity and wind speed and found that the peak2 event during 1996 is due to a cyclonic event. Further analysis with ENSO and IOD events shows that, during a positive IOD and La-Niña year, the observed annual average SWH and wind speed is comparatively lower whereas high SWH and wind speed are observed during a negative IOD and El-

Niño year and resulted in peak1. Whereas the peak3 was due to the locally formed low pressure event.

*Acknowledgements.* We thank the Director, CSIR-National Institute of Oceanography, Goa for providing the encouragement to carry out the study. This is NIO contribution No. 5505.

## References

Allan, J. and Komar, P.: Are ocean wave heights increasing in the eastern North Pacific?, EOS T. Am. Geophys. Un., 47, 566–567, 2000.

Ashok, K., Saji, N. H., and Yamagata, T.: Individual and combined influences of ENSO and Indian Ocean dipole on the Indian summer monsoon, J. Climate, 17, 3141–3155, 2004.

Berrisford, P., Dee, D., Fielding, K., Fuentes, M., Kållberg, K., Kobayashi, S., and Uppala, S.: The ERA-interim archive, ERA Report Series, 1, Technical Report, European Centre for Medium-Range Weather Forecasts, Shinfield Park, Reading, 16, 2009.

Bouws, E., Jannink, D., and Komen, G. J.: The increasing wave height in the North Atlantic Ocean, B. Am. Meteorol. Soc., 77, 2275–2277, 1996.

Caires, S. and Swail, V.: Global wave climate trend and variability analysis, 8th Int. Workshop on Wave Hind casting and Forecasting, 14–19 November, Oahu, Hawaii, US Army Engineer Research and Development Center's Coastal and Hydraulics Laboratory and Cosponsors, CD-ROM, AI, 2004.

Carter, D. J. T. and Draper, L.: Has the North East Atlantic become rougher?, Nature, 332, 494, doi:10.1038/332494a0, 1988.

Charles, E., Idier, D., Thiebot, J., Cozannet, G. L., Pedreros, R., Ardhuin, F., and Planton, S.: Present wave climate in the Bay of Biscay: spatiotemporal variability and trends from 1958–2001, J. Climate, 25, 2020–2039, 1988.

Dee, D. P. and Uppala, S.: Variational bias correction in ERA-Interim, ECMWF Tech. Rep. Memorandum, Reading, UK, 2008.

Dee, D. P., Uppala, S. M., Simmons, A. J., Berrisford, P., Poli, P., and Kobayashi, S.: The ERA-interim reanalysis: configuration and performance of the data assimilation system, Q. J. Roy. Meteor. Soc., 137, 553–597, 2011.

Dube, S. K., Rao, A. D., Sinha, P. C., Murty, T. S., and Bahulayan, N.: Numerical modelling of storm surges in the Arabian Sea, Appl. Math. Model., 9, 289–294, 1997.

Evan, A. T. and Camargo, S. J.: A Climatology of Arabian Sea Cyclonic Storms, J. Climate., 24, 140–158, 2011.

Glejin, J., Sanil Kumar, V., Balakrishnan Nair, T. M., and Singh, J.: Influence of winds on temporally varying short and long period gravity waves in the near shore regions of the eastern Arabian Sea, Ocean Sci., 9, 343–353, doi:10.5194/os-9-343-2013, 2013.

Gray, W. M.: Technical Document WMO/TD No. 72, WMO, Geneva, Switzerland, I, 3–19, 1985.

Gulev, S. K. and Grigorieva, V.: Last century changes in ocean wind wave height from global visual wave data, Geophys. Res. Lett., 31, L24302, doi:10.1029/2004GL021040, 2004.

Hemer, M. A., Church, J. A., and Hunter, J. R.: Variability and trends in the directional wave climate of the Southern Hemisphere, Int. J. Climatol., 30, 475–491, 2010.

Hemer, M. A., Fan, Y., Mori, N., Semedo, A., and Wang, X. L.: Projected changes in wave climate from a multi-model ensemble, Nature Climate Change, 3, 471–476, 2013.

Hirsch, R. M., Helsel, D. R., Cohn, T. A., and Gilroy, E. J.: Statistical analysis of hydrologic data, in: Handbook of Hydrology, edited by: Maidment, D. R., McGraw-Hill Inc., New York, 17, 17.11–17.37, 1993.

Jiang, Y., Luo, Y., Zhao, Z., and Tao, S.: Changes in wind speed over China during 1956–2004, Theor. Appl. Climatol., 99, 421–430, 2010.

Jury, M. R.: A preliminary study of climatological associations and characteristics of tropical cyclones in the southwest Indian Ocean, Meteorol. Atmos. Phys., 51, 101–115, 1993.

Kendall, M. G.: Rank Correlation Methods, Griffin, London, UK, 1975.

Krogstad, H. E. and Barstow, S. F.: Satellite wave measurements for coastal engineering applications, Coast. Eng., 37, 283–307, 1999.

Kumar, V. S.: Variation of wave directional spread parameters along the Indian coast, Appl. Ocean Res., 28, 98–103, 2006.

Kumar, V. S. and Sajiv, C.: Variations in long term wind speed during different decades in Arabian Sea and Bay of Bengal, J. Earth Syst. Sci., 119, 639–653, 2010.

Kumar, V. S., Kumar, K. A., and Anand, N. M.: Characteristics of waves off Goa, West coast of India, J. Coast. Res., 16, 782–789, 2000.

Kumar, V. S., Anand, N. M., Kumar, K. A., and Mandal, S.: Multipeakedness and groupiness of shallow water waves along Indian coast, J. Coast. Res., 19, 1052–1065, 2003.

Kumar, V. S., Singh, J., Pednekar, P., and Gowthaman, R.: Waves in the nearshore waters of northern Arabian Sea during the summer monsoon, Ocean Eng., 38, 382–388, 2011.

Kumar, V. S., Glejin, J., Dora, G. U., Sajiv, C. P., Singh, J., and Pednekar, P.: Variations in nearshore waves along Karnataka, west coast of India, J. Earth Sys. Sci., 121, 393–403, 2012.

Mann, H. B.: Nonparametric tests against trend, Econometrica, 13, 245–259, 1945.

McPhaden, M. J., Busalacchi, A. J., Cheney, R., Donguy, J. R., Gage, K. S., Halpern, D., Ji, M., Julian, P., Mayers, G., Mitchum, G. T., Niiler, P. P., Picaut, J., Reynolds, R. W., Smith, N., and Takeuchi, K.: The tropical ocean-global atmosphere (TOGA) observing system: a decade of progress, J. Geophys. Res., 103, 14169–14240, 1998.

Meyers, G., McIntosh, P., Pigot, L., and Pook, M.: The years of El-Niño, La-Niña and interactions with the tropical Indian Ocean, J. Climate, 20, 2872–2880, 2007.

Neu, H. J. A.: Interannual variations and longer-term changes in the sea state of the North Atlantic from 1970 to 1982, J. Geophys. Res., 89, 6397–6402, 1984.

OceanSITES: http://www.OceanSITES.org (last access: December 2009), 2009.

Praveen, K. B., Vialard, J., Lengaigne, M., Murty, V. S. N., McPhaden, M. J., Cronin, M., Pinsard, F., and Gopala Reddy, K.: TropFlux wind stresses over the tropical oceans: evaluation and comparison with other products, Clim. Dynam., 40, 2049–2071, 2013.

Premkumar, K., Ravichandran, M., Kalsi, S. R., Sengupta, D., and Gadgil, S.: First results from a new observation system over the Indian Seas, Curr. Sci. India, 78, 323–330, 2000.

Reason, C. J. C., Allan, R. J., Lindesay, J. A., and Ansell, T. J.: ENSO and climatic signals across the Indian Ocean Basin in the global context – Part 1: Interannual composite patterns, Int. J. Climatol., 20, 1285–1327, 2000.

Ruggiero, P., Komar, P., and Allan, J.: Increasing wave heights and extreme value projections: the wave climate of the US Pacific Northwest, Coast. Eng., 57, 539–552, 2010.

Saji, N. H. and Yamagata, T.: Structure of SST and surface wind variability during Indian ocean dipole mode events COADS observations, J. Climate, 16, 2735–2751, 2003.

Saji, N. H., Goswami, B. N., Vinayachandran, P. N., and Yamagata, T.: A dipole mode in the tropical Indian Ocean, Nature, 401, 360–363, 1999.

Sajiv, P. C., Kumar, V. S., Glejin, J., Dora, G. U., and Vinayaraj, P.: Interannual and seasonal variations in near shore wave characteristics off Honnavar, west coast of India, Curr. Sci. India, 103, 286–292, 2012.

Sanil Kumar, V., Sajiv Philip, C., and Balakrishnan Nair, T. N.: Waves in shallow water off west coast of India during the onset of summer monsoon, Ann. Geophys., 28, 817–824, doi:10.5194/angeo-28-817-2010, 2010.

Sen, P. K.: Estimates of the regression coefficient based on Kendall's tau, J. Am. Stat. Assoc., 63, 1379–1389, 1968.

Shyamala, B. and Iyer, B. G.: Statistical Study of Cyclonic Disturbances in Arabian Sea, Proceedings of TROPMET-1996, 14–17 February, Vishakhapatnam, 1996.

Simon, B., Joshi, P. C., Thapliyal, P. K., Pal, P. K., Sarkar, A., Bhatia, R. C., Jain, R. K., Singh, D., Mukherjee, S. K., and Gupta, H. V.: Monsoon onset-2000 monitored using multi-frequency microwave radiometer on-board Oceansat-1, Curr. Sci. India, 81, 647–651, 2001.

Singh, O. P.: Long term trends in the frequency of monsoonal cyclonic disturbances over the North Indian Ocean, Mausam, 52, 655–658, 2001.

Soomere, T. and Räämet, A.: Long-term spatial variations in the Baltic Sea wave fields, Ocean Sci., 7, 141–150, doi:10.5194/os-7-141-2011, 2011.

Srivastava, A. K., Sinha Ray, K. C., and De, U. S.: Trends in the frequency of cyclonic disturbances and their intensification over Indian seas, Mausam, 51, 113–118, 2000.

Theil, H.: A rank-invariant method of linear and polynomial regression analysis, International Proceedings of the Koninklijke Nederlandse Akademic van Wetenschappen Series, A53, 386–392, 1950.

Tucker, M. J. and Pitt, E. G.: Waves in Ocean Engineering, Elsevier ocean engineering book series, 5, 521 pp., Elsevier, Amsterdam, 2001.

Vanem, E., and Walker, S.-E.: Identifying trends in the ocean wave climate by time series analyses of significant wave height data, Ocean Eng., 61, 148–160, 2013.

Vinayachandran, P. N., Kurian, J., and Neema, C. P.: Indian Ocean response to anomalous conditions in 2006, Geophys. Res. Lett., 34, L15602, doi:10.1029/2007GL030194, 2007.

Webster, P. J., Moore, A. M., Loschnigg, J. P., and Leben, R. R.: Coupled ocean–atmosphere dynamics in the Indian Ocean during 1997–1998, Nature, 401, 356–360, 1999.

Xie, S. P., Annamalai, H., Schott, F. A., and McCreary Jr., J. P.: Structure and mechanisms of south Indian Ocean climate variability, J. Climate, 15, 864–878, 2002.

Yamagata, T., Behera, S. K., Rao, S. A., Guan, Z., Ashok, K., and Saji, N. H.: The Indian Ocean dipole: A physical entity, CLIVAR Exchanges, 24, 15–18, 2002.

Young, I. R., Zieger, S., and Babanin, A.: Global trends in wind speed and wave height, Science, 332, 451–455, 2011.

Yuan, J. and Cao, J.: North Indian Ocean tropical cyclone activities influenced by the Indian Ocean dipole mode, Sci. China Ser. D, 56, 1–11, 2012.

**Table 1.** Trend of wind speed and significant wave height (SWH) during 1979–2012 in different months.

| Month | Wind speed ($\mathrm{cm\,s^{-1}\,yr^{-1}}$) | | SWH ($\mathrm{cm\,yr^{-1}}$) | |
|---|---|---|---|---|
| | Mean | Max | Mean | Max |
| Jan | −0.518 | 1.426 | −0.044 | 0.378 |
| Feb | −1.318 | −2.645 | −0.321 | −0.153 |
| Mar | −2.234 | −2.437 | −0.402 | −0.374 |
| Apr | −2.340 | −3.224 | −0.417 | −0.194 |
| May | −0.830 | 2.316 | 0.274 | 1.483 |
| Jun | −2.771 | −0.789 | 0.138 | 1.045 |
| Jul | −1.258 | −2.578 | 0.791 | 0.692 |
| Aug | −3.817 | −0.079 | −0.550 | 0.111 |
| Sep | −0.137 | 6.140 | 0.907 | 1.987 |
| Oct | −0.886 | −2.204 | 0.028 | 0.393 |
| Nov | −1.160 | 1.498 | −0.206 | 0.418 |
| Dec | −0.418 | 1.035 | −0.084 | 0.034 |

**Table 2.** Frequency of occurrence of wind speed in different decades.

| Wind speed range ($\mathrm{m\,s^{-1}}$) | Frequency (%) | | |
|---|---|---|---|
| | 1980–1989 | 1990–1999 | 2000–2009 |
| 0–3 | 30.89 | 34.40 | 38.68 |
| 3–6 | 54.55 | 51.15 | 49.96 |
| 6–9 | 13.61 | 13.43 | 10.46 |
| 9–12 | 0.90 | 0.98 | 0.84 |
| > 12 | 0.05 | 0.05 | 0.05 |

**Table 3.** Student *t* test and *Z* test for wave and wind.

| Parameter | *T* test | | | *Z* test | | |
|---|---|---|---|---|---|---|
| | $\alpha$-level | *P* value (two tailed) | 95 % confidence interval on the mean: | Standard deviation | *P* value | 95 % confidence interval on the mean: |
| SWH_mean | 5 % | $< 0.0001$ | (1.227, 1.249) | 0.031 | $< 0.0001$ | (1.228, 1.248) |
| SWH_max | 5 % | $< 0.0001$ | (3.532, 3.985) | 0.650 | $< 0.0001$ | (3.54, 3.94) |
| Wind speed_mean | 5 % | $< 0.0001$ | (3.816, 3.954) | 0.198 | $< 0.0001$ | (3.818, 3.951) |
| Wind speed_max | 5 % | $< 0.0001$ | (10.780, 12.148) | 1.99 | $< 0.0001$ | (10.806, 12.148) |

Title Page
Abstract Introduction
Conclusions References
Tables Figures
◀◀ ▶▶
◀ ▶
Back Close
Full Screen / Esc
Printer-friendly Version
Interactive Discussion

**Table 4.** Mann–Kendall significance test for trend analysis.

| Parameter | Variance | Man | Standard deviation | Mann–Kendall test | | |
|---|---|---|---|---|---|---|
| | | | | Sen's slope | *P* value (two tailed) | Significance |
| SWH_mean | 0.0009 | 1.238 | 0.031 | 0.0001 | 0.7 | NS |
| SWH_max | 0.422 | 3.758 | 0.650 | 0.016 | 0.16 | NS |
| SWH 90th percentile | 1.67 | 2.58 | 1.29 | 0.0016 | 0.49 | NS |
| SWH 99th percentile | 1.67 | 3.47 | 1.34 | 0.008 | 0.15 | NS |
| Wind speed mean | 0.039 | 3.885 | 0.198 | −0.014 | 0.0001 | SG |
| Wind speed max | 3.99 | 11.47 | 1.99 | 0.020 | 0.40 | NS |
| Wind speed 90th percentile | 0.096 | 6.4 | 0.31 | −0.018 | 0.0001 | SG |
| Wind speed 99th percentile | 0.38 | 8.95 | 0.62 | −0.019 | 0.12 | NS |

Title Page
Abstract
Introduction
Conclusions
References
Tables
Figures
◂◂
▸▸
◂
▸
Back
Close
Full Screen / Esc
Printer-friendly Version
Interactive Discussion

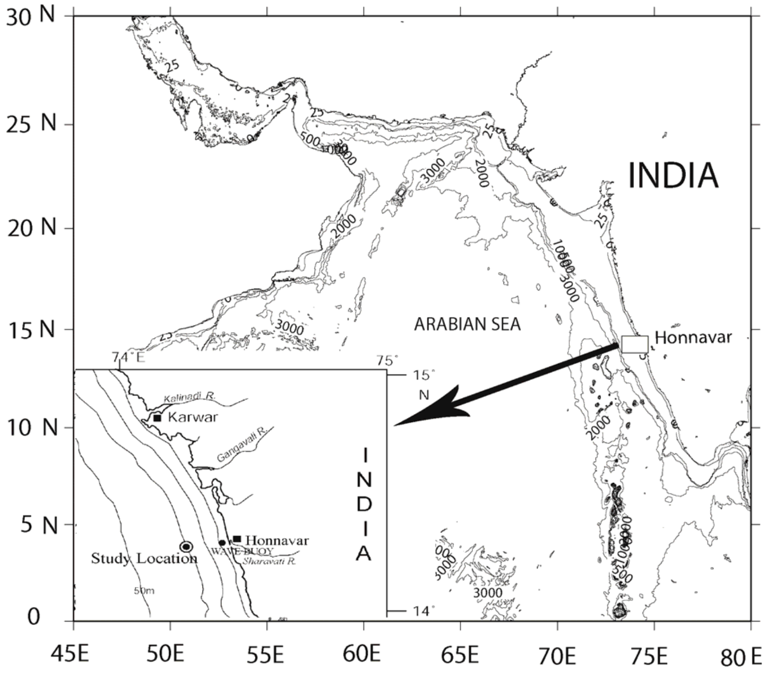

**Fig. 1.** Study area along with location of extracted model dataset and buoy.

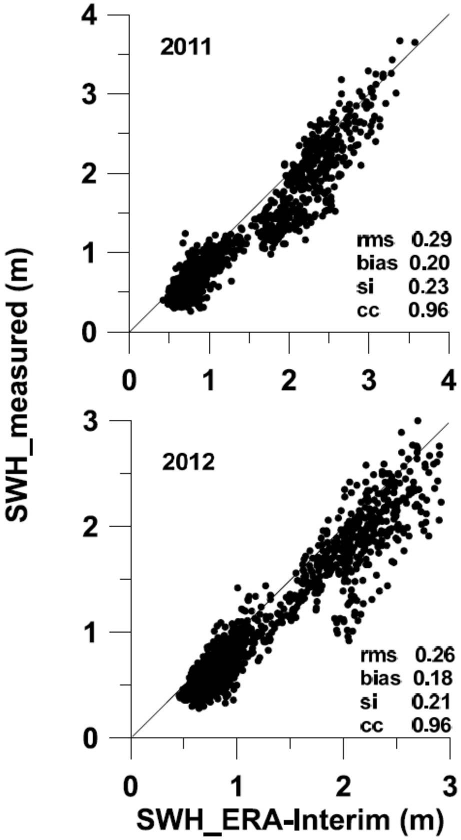

**Fig. 2.** Scatter plot showing the comparison of wave parameters (significant wave height, zero crossing wave period and energy wave period) based on ERA-Interim and in-situ buoy data during 2011 and 2012.

Title Page

Abstract | Introduction

Conclusions | References

Tables | Figures

◀| |▶

◀ ▶

Back | Close

Full Screen / Esc

Printer-friendly Version

Interactive Discussion

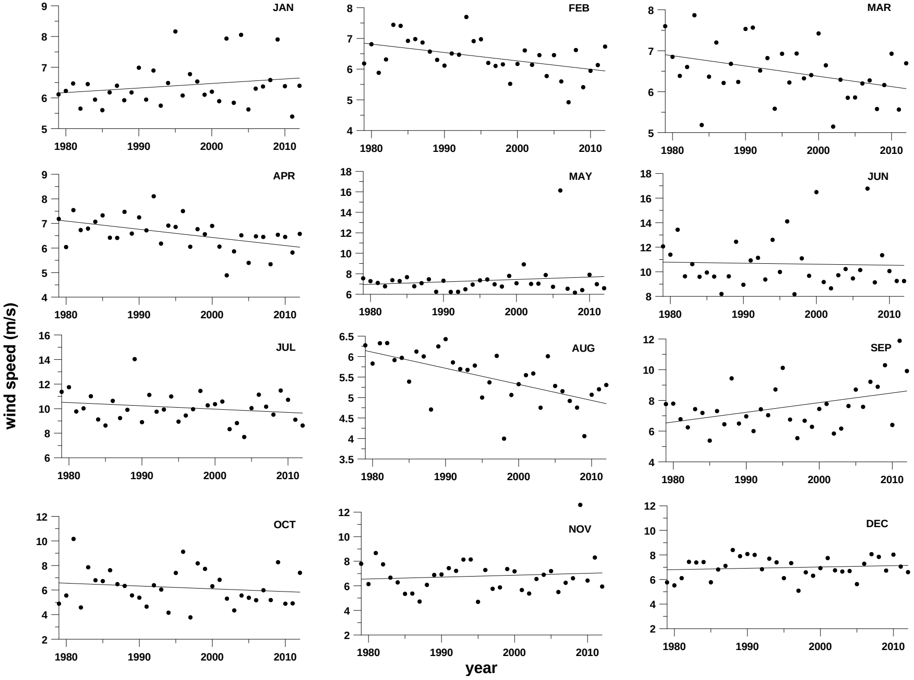

**Fig. 3.** Temporal variation of monthly maximum of wind speed during 1979–2012.

Title Page
Abstract | Introduction
Conclusions | References
Tables | Figures
◀◀ | ▶▶
◀ | ▶
Back | Close
Full Screen / Esc
Printer-friendly Version
Interactive Discussion

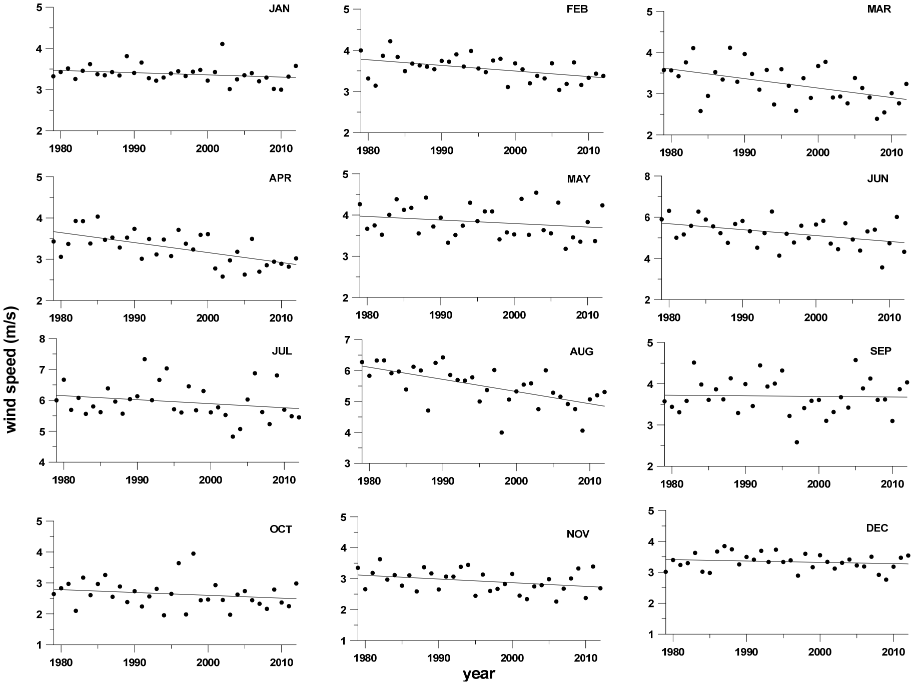

Fig. 4. Temporal variation of monthly average wind speed during 1979–2012.

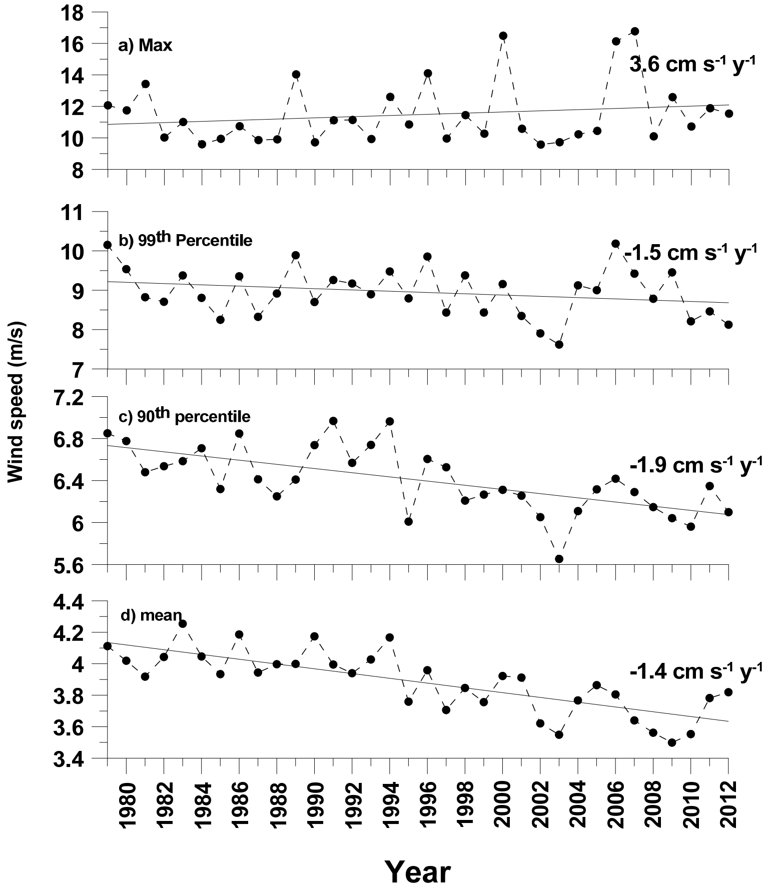

**Fig. 5.** Long term trend in annual **(a)** maximum, **(b)** 99th percentile, **(c)** 90th percentile and **(d)** mean wind speed during 1979–2012.

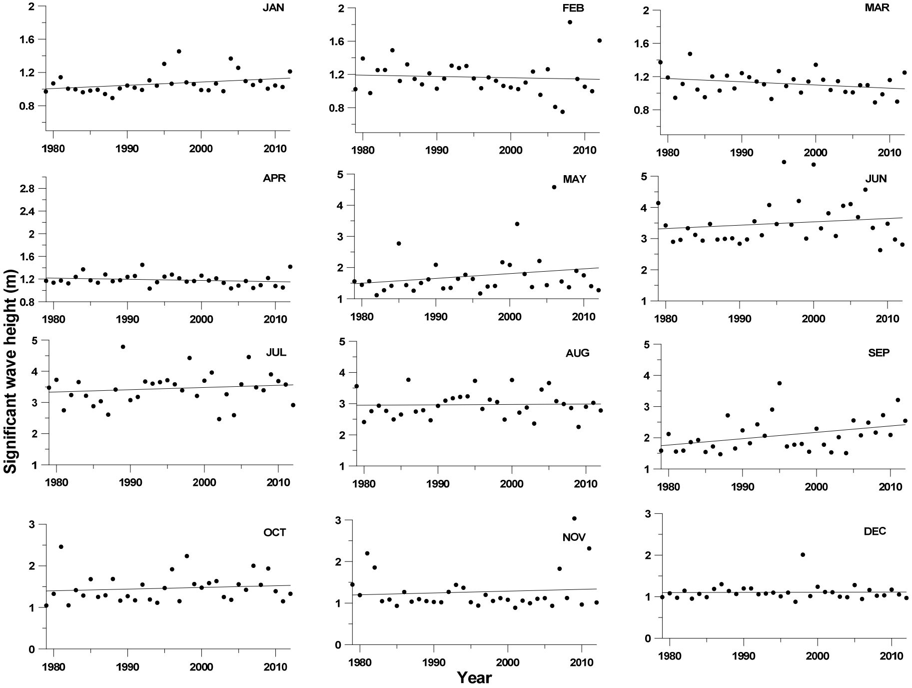

**Fig. 6.** Temporal variation of monthly maximum significant wave height during 1979–2012.

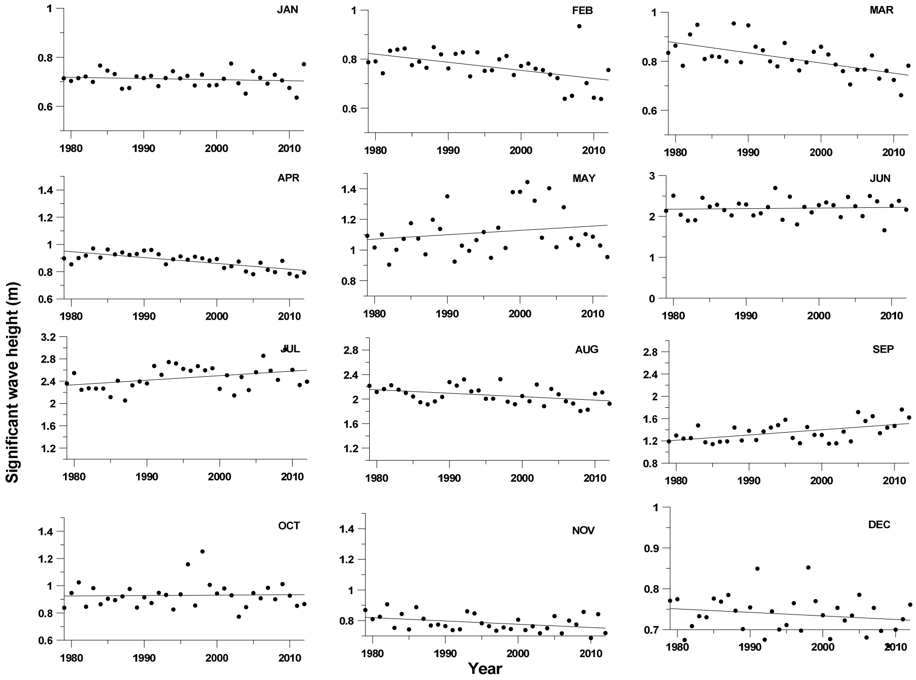

**Fig. 7.** Temporal variation of monthly mean significant wave height during 1979–2012.

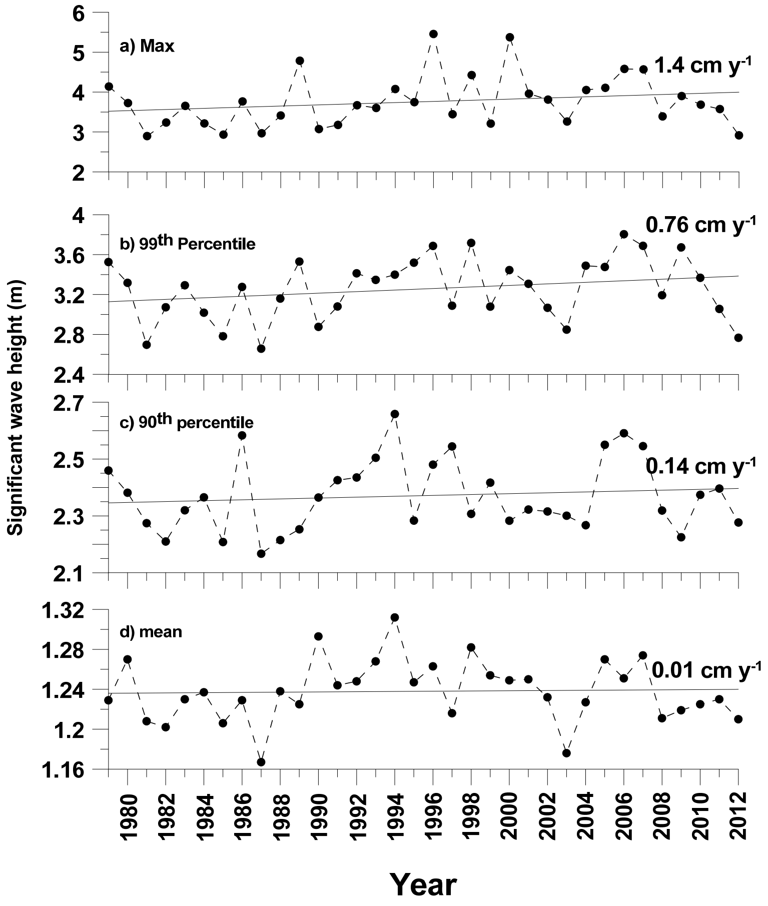

**Fig. 8.** Long term trend in annual **(a)** maximum, **(b)** 99th percentile, **(c)** 90th percentile and **(d)** mean significant wave height during 1979–2012.

Title Page
Abstract
Introduction
Conclusions
References
Tables
Figures
◀◀
▶▶
◀
▶
Back
Close
Full Screen / Esc
Printer-friendly Version
Interactive Discussion

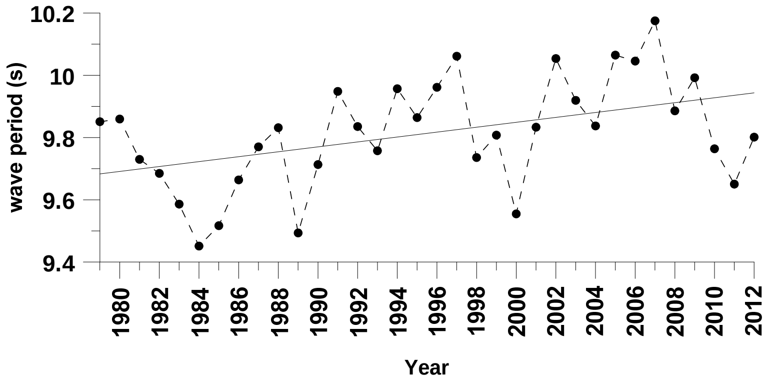

**Fig. 9.** Variation of annual 90th percentile energy wave period during 1979–2012.

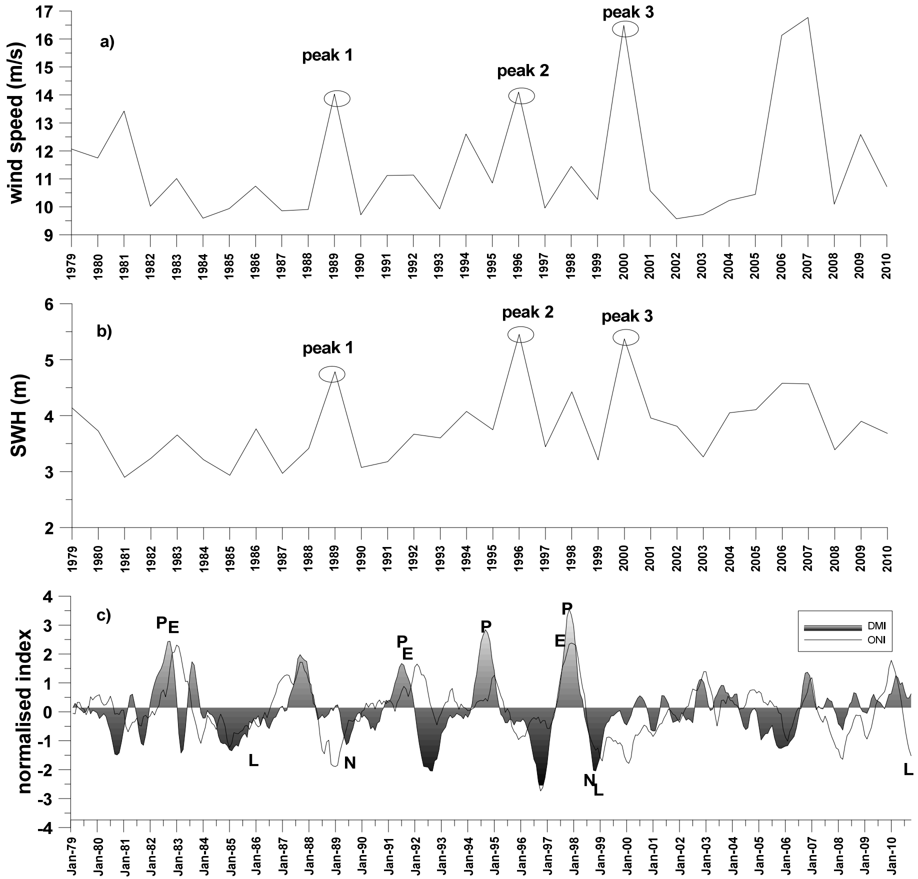

**Fig. 10.** Temporal variation of **(a)** annual maximum wind speed **(b)** annual maximum SWH and **(c)** Oceanic Nino Index and Dipole Mode Index during 1979–2010 (P denotes strong positive IOD year, N – negative IOD year, E – El-Niño year, L – La-Niña year).

Title Page
Abstract
Introduction
Conclusions
References
Tables
Figures
|◀
▶|
◀
▶
Back
Close
Full Screen / Esc
Printer-friendly Version
Interactive Discussion